

University of Massachusetts Medical School

eScholarship@UMMS

Open Access Articles

Open Access Publications by UMMS Authors

2018-10-08

TIP55, a splice isoform of the KAT5 acetyltransferase, is essential for developmental gene regulation and organogenesis

Diwash Acharya

University of Massachusetts Medical School

Et al.

Let us know how access to this document benefits you.

Follow this and additional works at: <https://escholarship.umassmed.edu/oapubs>



Part of the [Amino Acids, Peptides, and Proteins Commons](#), [Cell Biology Commons](#), [Cells Commons](#), [Developmental Biology Commons](#), [Enzymes and Coenzymes Commons](#), and the [Genetic Phenomena Commons](#)

Repository Citation

Acharya D, Nera B, Milstone ZJ, Bourke L, Yoon Y, Rivera-Pérez JA, Trivedi CM, Fazio TG. (2018). TIP55, a splice isoform of the KAT5 acetyltransferase, is essential for developmental gene regulation and organogenesis. Open Access Articles. <https://doi.org/10.1038/s41598-018-33213-4>. Retrieved from <https://escholarship.umassmed.edu/oapubs/3633>

Creative Commons License



This work is licensed under a [Creative Commons Attribution 4.0 License](#).

This material is brought to you by eScholarship@UMMS. It has been accepted for inclusion in Open Access Articles by an authorized administrator of eScholarship@UMMS. For more information, please contact Lisa.Palmer@umassmed.edu.

SCIENTIFIC REPORTS



OPEN

TIP55, a splice isoform of the KAT5 acetyltransferase, is essential for developmental gene regulation and organogenesis

Diwash Acharya¹, Bernadette Nera¹, Zachary J. Milstone^{2,3}, Lauren Bourke^{1,2,3}, Yeonsoo Yoon⁴, Jaime A. Rivera-Pérez⁴, Chinmay M. Trivedi^{1,2,3} & Thomas G. Fazzio¹

Regulation of chromatin structure is critical for cell type-specific gene expression. Many chromatin regulatory complexes exist in several different forms, due to alternative splicing and differential incorporation of accessory subunits. However, *in vivo* studies often utilize mutations that eliminate multiple forms of complexes, preventing assessment of the specific roles of each. Here we examined the developmental roles of the TIP55 isoform of the KAT5 histone acetyltransferase. In contrast to the pre-implantation lethal phenotype of mice lacking all four *Kat5* transcripts, mice specifically deficient for *Tip55* die around embryonic day 11.5 (E11.5). Prior to developmental arrest, defects in heart and neural tube were evident in *Tip55* mutant embryos. Specification of cardiac and neural cell fates appeared normal in *Tip55* mutants. However, cell division and survival were impaired in heart and neural tube, respectively, revealing a role for TIP55 in cellular proliferation. Consistent with these findings, transcriptome profiling revealed perturbations in genes that function in multiple cell types and developmental pathways. These findings show that *Tip55* is dispensable for the pre- and early post-implantation roles of *Kat5*, but is essential during organogenesis. Our results raise the possibility that isoform-specific functions of other chromatin regulatory proteins may play important roles in development.

Regulation of chromatin structure is necessary to establish and maintain cell type-specific gene expression patterns during development. Generation of active or repressive chromatin architecture at gene enhancers and promoters is necessary for the binding and activities of lineage specific transcription factors^{1,2}. On a broader scale, large chromosomal domains of active or repressive chromatin structure help to enforce gene expression patterns particular to each cell lineage³. Consequently, mutations in subunits of chromatin remodeling factors—multisubunit protein complexes that regulate chromatin architecture through a range of enzymatic activities—frequently result in developmental abnormalities⁴.

The lysine acetyltransferase KAT5 (originally named TIP60) is conserved throughout eukaryotes and activates gene expression through acetylation of histones H2A (and H2A variants), H4, and numerous transcription factors^{5–9}. The KAT5 acetyltransferase activity is also necessary for the cellular response to DNA damage, in part by remodeling chromatin structure near sites of DNA damage^{7,8,10–12}. Interestingly, KAT5 also has an essential non-catalytic role in regulation of chromatin accessibility and gene expression in embryonic stem cells and pre-implantation embryos¹³. KAT5 is a component of the 17-subunit TIP60-P400 complex, which remodels chromatin architecture not only through acetylation of histone tails, but also through incorporation of the H2A.Z histone variant into nucleosomes. Previously, individual knockdown of multiple subunits of TIP60-P400 resulted in loss of embryonic stem cell self-renewal, as well as a defect in differentiation^{14,15}. Consistent with these

¹Department of Molecular, Cell, and Cancer Biology, University of Massachusetts Medical School, Worcester, MA, 01605, USA. ²Division of Cardiovascular Medicine, University of Massachusetts Medical School, Worcester, MA, 01605, USA. ³Department of Medicine, University of Massachusetts Medical School, Worcester, MA, 01605, USA. ⁴Department of Pediatrics, Division of Genes and Development, University of Massachusetts Medical School, Worcester, MA, 01605, USA. Diwash Acharya and Bernadette Nera contributed equally. Correspondence and requests for materials should be addressed to T.G.F. (email: thomas.fazzio@umassmed.edu)

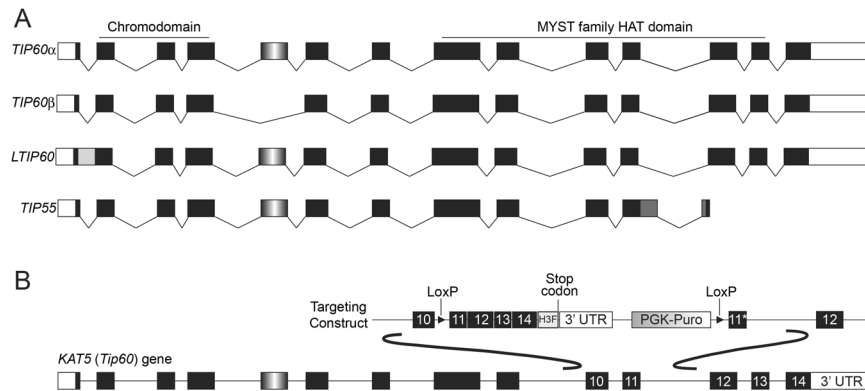


Figure 1. Four splice variants are expressed from the *Kat5* locus. **(A)** Variants of *Kat5* mRNA produced by alternative splicing. Black boxes: coding regions within exons; white boxes: non-coding sequences within exons; black lines: spliced introns; gray boxes: in frame intronic regions retained in specific *Kat5* isoforms; gradient filled box: exon 5, which is spliced out in the *Tip60β* isoform. **(B)** Targeting construct used to generate both catalytically inactive *Kat5* mutant mice¹³ and *Tip55* knockout mice (described herein). The *Tip55* allele was made by removing the intronic regions retained selectively in *Tip55* and fusing the remaining exons (which are all included in all other *Kat5* isoforms).

phenotypes, mice with homozygous null mutations of the *Kat5* gene arrest development at E3.5, prior to implantation, and *Kat5*^{-/-} blastocysts fail to hatch from the zona pellucida when cultured *in vitro*¹⁶.

Although most studies of *Kat5* functions have focused on a single isoform, denoted *Tip60α*, several isoforms are expressed in mouse and human by virtue of alternative splicing. Four isoforms are expressed in mouse, *Tip60α*, *Tip60β*, *LTIP60*, and *Tip55*, which differ by alternative inclusion of intron 1, exon 5, or a portion of intron 11 combined with early termination of the reading frame (Fig. 1A)^{17–19}. The amino acid sequences of *LTIP60* and *Tip55* differ from *TIP60α* and *TIP60β* near or within the critical chromodomain and MYST domain, respectively, raising the possibility that these sequence alterations affect their functions. The *Kat5* gene is broadly expressed throughout development, although it is unclear which isoforms are expressed in each tissue, owing to a lack of reagents for distinguishing the different isoproteins. Therefore, the extent to which each *Kat5* isoform functions specifically or redundantly with other isoforms is currently unknown.

Here we test the hypothesis that *Tip55* acts non-redundantly in development by specifically mutating this isoform within the mouse *Kat5* gene. We show that *Tip55* is necessary for embryonic development, with *Tip55* homozygous mutant animals dying at or around E11.5. Prior to the appearance of overt developmental phenotypes, we observe defects in both heart and neural tube, which manifest as defects in cellular proliferation and increased cell death. Transcriptomic analyses of embryos prior to the appearance of developmental defects reveal alterations in developmental pathways that contribute to numerous tissues and organ systems. These data reveal a critical function of *Tip55* in organogenesis that is distinct from the early, pre-implantation defect observed when all four *Kat5* isoforms are lost and raise the possibility that additional isoforms of *Kat5* have unique, non-redundant functions during development.

Results

***Tip55* is essential for embryonic development.** The *TIP55* protein lacks the C-terminal 124 amino acids of the other three *KAT5* isoforms, *TIP60α*, *TIP60β*, and *LTIP60*. In its place, *TIP55* has a unique 103 amino acid C-terminus encoded by a portion of intron 11¹⁷ (Fig. 1A). This unique C-terminal region lacks amino acid sequence features of any well-established protein domain. We previously generated a multifunctional *Kat5* mutant mouse that specifically eliminates the *Tip55* isoform and can be converted to a catalytically inactive *Kat5* allele upon Cre-mediated recombination. To generate the *Tip55* null mutation, we deleted introns 11, 12, and 13, fusing exons 11–14, and in the process removing the region encoding the unique 103 amino acids of *TIP55* (Fig. 1B). This allele eliminates *Tip55* expression, but does not alter the coding sequence or expression of the remaining isoforms (Fig. 1A, Fig. S1A–C), which are able to form normal *TIP60*-*P400* complexes¹³. We previously examined the role of the *Kat5* lysine acetyltransferase (KAT) activity after Cre-mediated recombination of the *Tip55* KO cassette, and found that these KAT-deficient mutant mice progress beyond pre-implantation stages but exhibit defects at or before gastrulation¹³. However, the question of whether *Tip55* is required at any stage of development has not been addressed.

To test this possibility, we intercrossed mice heterozygous for the *Tip55* mutant allele (hereafter, *Tip55*^{Δ/+}) to generate *Tip55*^{Δ/Δ} homozygotes. We recovered no *Tip55*^{Δ/Δ} pups at birth ($\chi^2 = 38.05$; $P < 0.0001$), suggesting that the *Tip55* isoform is essential for embryonic development (Fig. 2A). To determine the stage at which embryonic development of *Tip55*^{Δ/Δ} mice was blocked, we dissected and genotyped embryos from E8.5 to E11.5. No overt phenotype was apparent at E8.5 (Fig. 2B). In contrast, *Tip55*^{Δ/Δ} embryos were smaller than *Tip55*^{+/+} or *Tip55*^{Δ/+} at E9.5, although they appeared morphologically normal (Fig. 2B). Although *Tip55*^{Δ/Δ} embryos could readily be recovered as late as E10.5 and occasionally as late as E11.5 (Fig. 2A), all E11.5 *Tip55*^{Δ/Δ} embryos lacked beating hearts, suggesting a potential cause of death. The lack of *Tip55* expression in *Tip55*^{Δ/Δ} homozygotes was confirmed by RT-PCR (Fig. S1). These data reveal that, unlike null mutants lacking all *Kat5* isoforms or *Kat5*

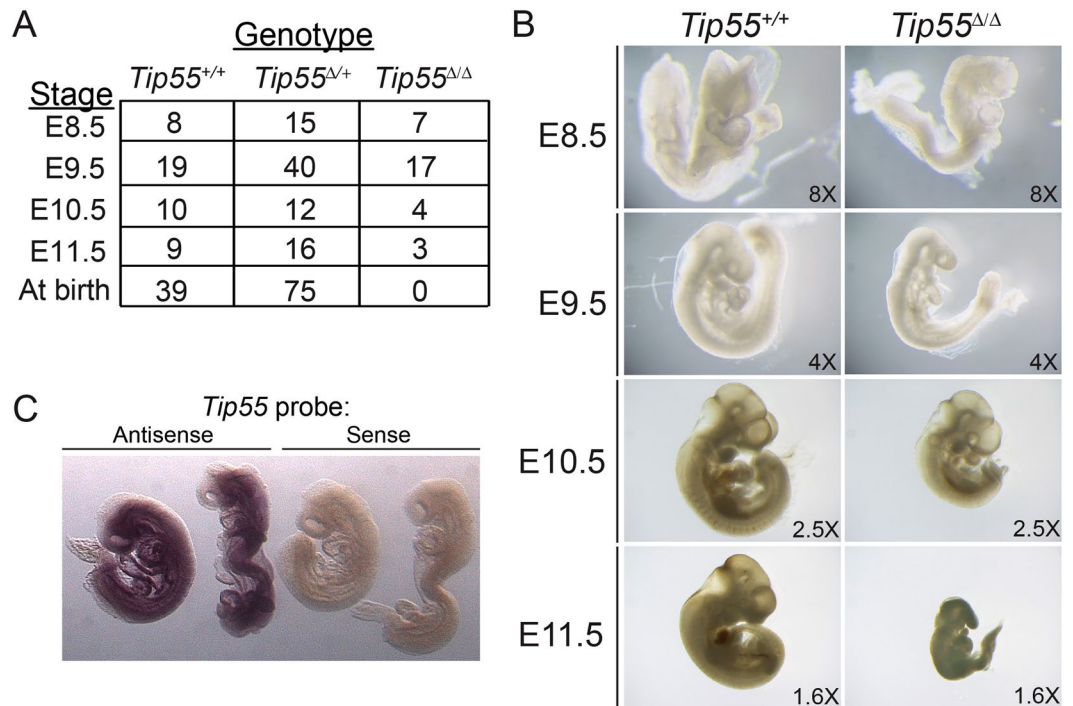


Figure 2. *Tip55* homozygous knockout mice die at or before embryonic day 11.5. **(A)** Genotypes of embryos recovered at indicated stages of development or at birth. **(B)** Representative images of wild type (*Tip55*^{+/+}) and knockout (*Tip55*^{Δ/Δ}) embryos at stages indicated. Different magnifications as indicated (lower right) were required to image embryos at each stage, owing to differences in size. **(C)** Whole-mount *in situ* hybridization of *Tip55* transcript. Shown are wild type E8.5–E9.0 mouse embryos hybridized with antisense or sense (as a negative control) *in situ* hybridization probes corresponding to the region of intron 11 retained in the *Tip55* transcript but not found in all other *Kat5* isoforms.

KAT-deficient mutants, *Tip55*^{Δ/Δ} mice progress normally through early pre- and post-implantation developmental stages. However, *Tip55*^{Δ/Δ} mice die during mid-gestation, potentially due to a fully penetrant defect in heart development.

***Tip55* is required for development of the heart and neural tube.** Key early steps in organogenesis, including formation of the heart tube and closure of the neural tube, occur at approximately embryonic day 8 of mouse development, shortly before developmental defects are apparent in *Tip55*^{Δ/Δ} embryos. To investigate the possibility that *Tip55*^{Δ/Δ} embryos are defective in some aspects of organ formation, we first tested whether *Tip55* was expressed in normal embryos at the initial stages of organogenesis. We performed RT-qPCR for *Tip55*, as well as for two additional *Tip60* isoforms for which specific primers could be designed, *LTip60* and *Tip60β*, using RNA isolated from E7.5–E11.5 embryos. We observed *Tip55* expression at all stages, albeit to lower levels than observed for the other isoforms (Fig. S2). Furthermore, using whole-mount *in situ* hybridization and an intron 11 probe specific for the *Tip55* isoform (dark gray boxes in Fig. 1A), we observed that expression of *Tip55* was widespread in E8.5–E9.0 embryos (Fig. 2C).

Next, we examined several features of *Tip55*^{+/+} and *Tip55*^{Δ/Δ} embryos at E8.5 (prior to the appearance of developmental defects in *Tip55*^{Δ/Δ} mutants) in embryo sections. We observed no obvious differences in organization of the body plan in sagittal sections of multiple embryos of each genotype (Fig. 3A). We performed immunohistochemistry with antibodies against Histone H3 phosphorylated at serine 10 (H3S10P) or cleaved caspase 3 (CC3) to test for proliferating or apoptotic cells, respectively. Although most regions of *Tip55*^{Δ/Δ} embryos were normal, the proportion of H3S10P positive cells was significantly reduced in heart, whereas cleaved caspase 3 staining was significantly elevated in neural tube (Fig. 3B–D). (Cleaved caspase 3 staining also appeared to be higher in heart in *Tip55*^{Δ/Δ} embryos, but the differences were not statistically significant.) These data suggest that loss of *Tip55* results in defects in proliferation and/or increased apoptosis in multiple organs and further suggest that embryonic lethality caused by this mutation is due to defects in organ development.

We next examined whether the observed phenotypes were associated with a failure to specify the heart and neural lineages. To test this possibility, we performed immunofluorescence staining of wild type and mutant embryo sections for markers of neural lineage (SOX2) and cardiac muscle (cardiac troponin T, cTNT). As above, we stained sections from E8.5 embryos to minimize indirect effects of developmental arrest. However, we observed no difference in staining of either marker in *Tip55* mutant embryos relative to wild type (Fig. S3). These data suggest that *Tip55* loss impairs proliferation and viability of cardiac and neural progenitor cells downstream of cell type specification in both organs.

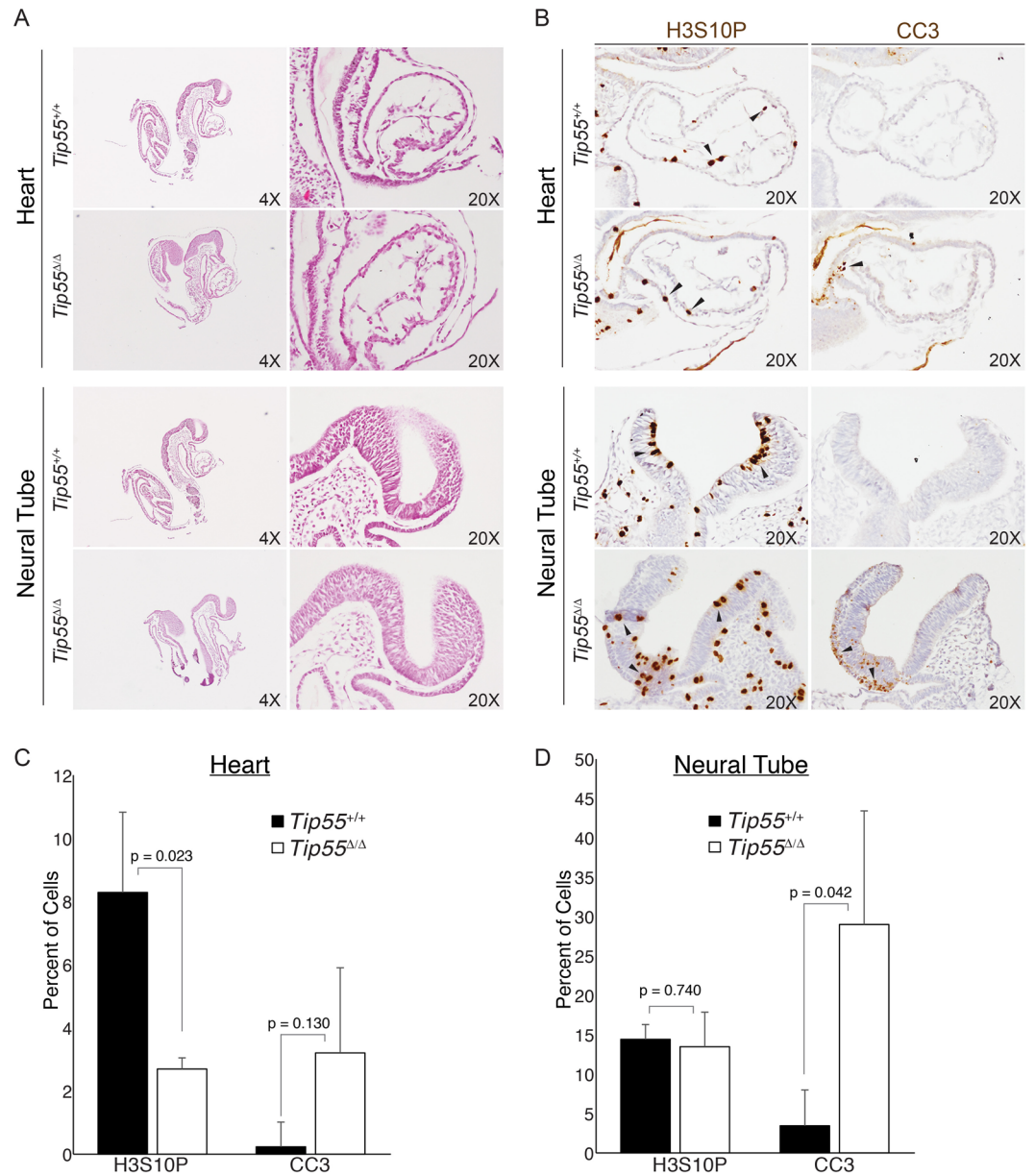


Figure 3. *Tip55* loss leads to defects in heart and neural tube. **(A)** Hematoxylin and Eosin (H&E) stained E8.5 embryo sections of *Tip55*^{+/+} and *Tip55*^{Δ/Δ} embryos, shown at multiple magnifications to reveal overall morphology (4X) or focus on heart (20X, above) and neural tube (20X, below). **(B)** Immunohistochemistry staining of cleaved caspase 3 (CC3) or Histone H3 phosphorylated on serine 10 (H3S10P) on E8.5 sections of *Tip55*^{+/+} and *Tip55*^{Δ/Δ} embryos. Examples of positively staining cells denoted with arrowheads. **(C,D)** Quantification of cells staining positively for each H3S10P and CC3 in heart **(C)** and neural tube **(D)**. N = 3 embryo sections were used. P-values were calculated using a two-sided t-test.

***Tip55* is required for proliferation of MEFs *ex vivo*.** The reduced H3S10P staining of *Tip55*^{Δ/Δ} embryos in E8.5 heart suggested that TIP55 may promote cellular proliferation. However, a reduction in the number of proliferating cells could also result indirectly from increased cell death or other defects. Therefore, to directly test whether TIP55 was necessary for proliferation, we measured the proliferation rate and morphology of cells isolated from embryos with and without *Tip55* mutations. Fibroblasts (MEFs) were isolated from *Tip55*^{+/+}, *Tip55*^{+/-}, and *Tip55*^{Δ/Δ} embryos and cultured during a four-day time course. We found that *Tip55*^{Δ/Δ} MEFs proliferated minimally after isolation at E9.5, followed by growth arrest shortly thereafter (Fig. 4A). Furthermore, *Tip55*^{Δ/Δ} MEFs exhibited flattened and elongated cell morphology reminiscent of cells undergoing senescence, in contrast to *Tip55*^{+/+} and *Tip55*^{+/-} cells (Fig. 4B). Indeed, *Tip55*^{Δ/Δ} MEFs exhibited modest but reproducibly elevated staining for senescence-associated β -galactosidase activity compared to *Tip55*^{+/+} and *Tip55*^{+/-} MEFs (Fig. 4B). Together, these data suggest that *Tip55* is required for the proliferation of some embryonic cell types and suppression of cellular senescence.

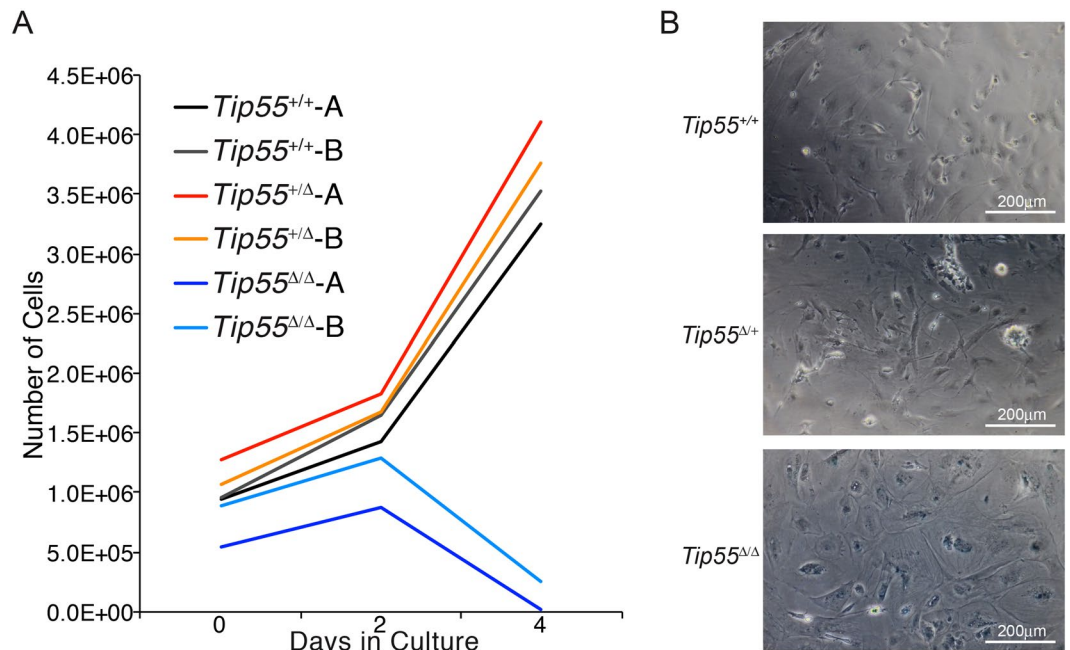


Figure 4. *Tip55* mutant MEFs exhibit premature proliferation arrest. **(A)** Growth curve indicating numbers of cells of each genotype after growth in culture for indicated lengths of time. Cells were seeded at approximately equivalent densities. **(B)** Bright field images of mouse embryonic fibroblasts (MEFs) isolated from mouse embryos with the indicated genotypes and stained for β -galactosidase activity (blue) after five days of culture. Scale bars are indicated.

Drivers of organ and tissue development are misregulated in *Tip55*^{Δ/Δ} mice. *Kat5* isoforms act in part by acetylation of the N-terminal tails of histones H2A and H4 near gene regulatory regions, which promotes transcription¹⁰. To test whether genes required for development, cellular proliferation, or other processes were misregulated upon loss of the *Tip55* isoform, we isolated RNA from *Tip55*^{+/+} or *Tip55*^{Δ/Δ} embryos at E8.5, prior to the appearance of morphological defects in *Tip55*^{Δ/Δ} embryos (Fig. 2B), and performed RNA-seq. We observed strong concordance among three biological replicates for *Tip55*^{+/+} and *Tip55*^{Δ/Δ} (Fig. 5A,B). Next, we used EBseq analysis²⁰ to identify genes that are significantly differentially expressed in *Tip55*^{Δ/Δ} embryos. We identified 2507 genes that were significantly misregulated in *Tip55*^{Δ/Δ} embryos (posterior probability of differential expression, PPDE > 0.95), with 278 of those genes misregulated more than two-fold (Fig. 5C and Table S1). We validated several differentially expressed genes by RT-qPCR and observed results consistent with the RNA-seq data (Fig. 5D).

To uncover classes of genes significantly misregulated in *Tip55*^{Δ/Δ} embryos, we identified Gene Ontology (GO) terms significantly enriched among the differentially expressed genes. These analyses demonstrated that the differentially expressed genes were highly enriched for developmental regulators and genes required for development of multiple tissue types, including blood, muscle, and brain (Fig. 5E,F). *Kat5* is necessary for proper silencing of a number of developmental regulators in embryonic stem cells¹³. Therefore, genes upregulated in *Tip55*^{Δ/Δ} embryos may include some that are repressed by TIP55. In addition, developmental delays in *Tip55*^{Δ/Δ} embryos may cause expression of genes that peak early in wild type embryos (and normally exhibit reduced expression by E8.5) to be more highly expressed in *Tip55*^{Δ/Δ} mutants at E8.5 as a result of their delayed or extended window of expression.

Among numerous developmentally regulated genes that were downregulated in *Tip55*^{Δ/Δ} embryos were factors that promote blood cell development – including key erythroid factors *Gata1* and *Klf1* – suggesting *Tip55* loss leads to a failure to initiate erythropoiesis. However, these data do not distinguish whether the effect of *Tip55*^{Δ/Δ} on erythroid development is due to a direct role for TIP55 at the regulatory regions of key erythroid regulators or an indirect effect on gene expression due to other developmental abnormalities (such as in heart). In sum, we conclude that *Tip55* is necessary in multiple cell and tissue types for normal expression of differentiation genes that are critical for organ development.

Discussion

Here we have shown an essential, non-redundant role of the *Tip55* isoform of *Kat5* during post-implantation embryonic development. These findings contrast with the phenotype of a mouse mutant that lacks all four *Kat5* transcripts, which causes pre-implantation lethality at the blastocyst stage¹⁶, as well as a KAT-deficient mutant that exhibits defects in gastrulation¹³. The defects of *Tip55*^{Δ/Δ} embryos in formation of heart and neural tube suggest this mutation impairs development of multiple cell lineages, a finding that is verified by our transcriptomic data indicating mis-expression of developmental regulators of multiple tissue types. On a cellular level, *Tip55*^{Δ/Δ} results in a combination of reduced proliferation and increased apoptosis in several different tissues and cell

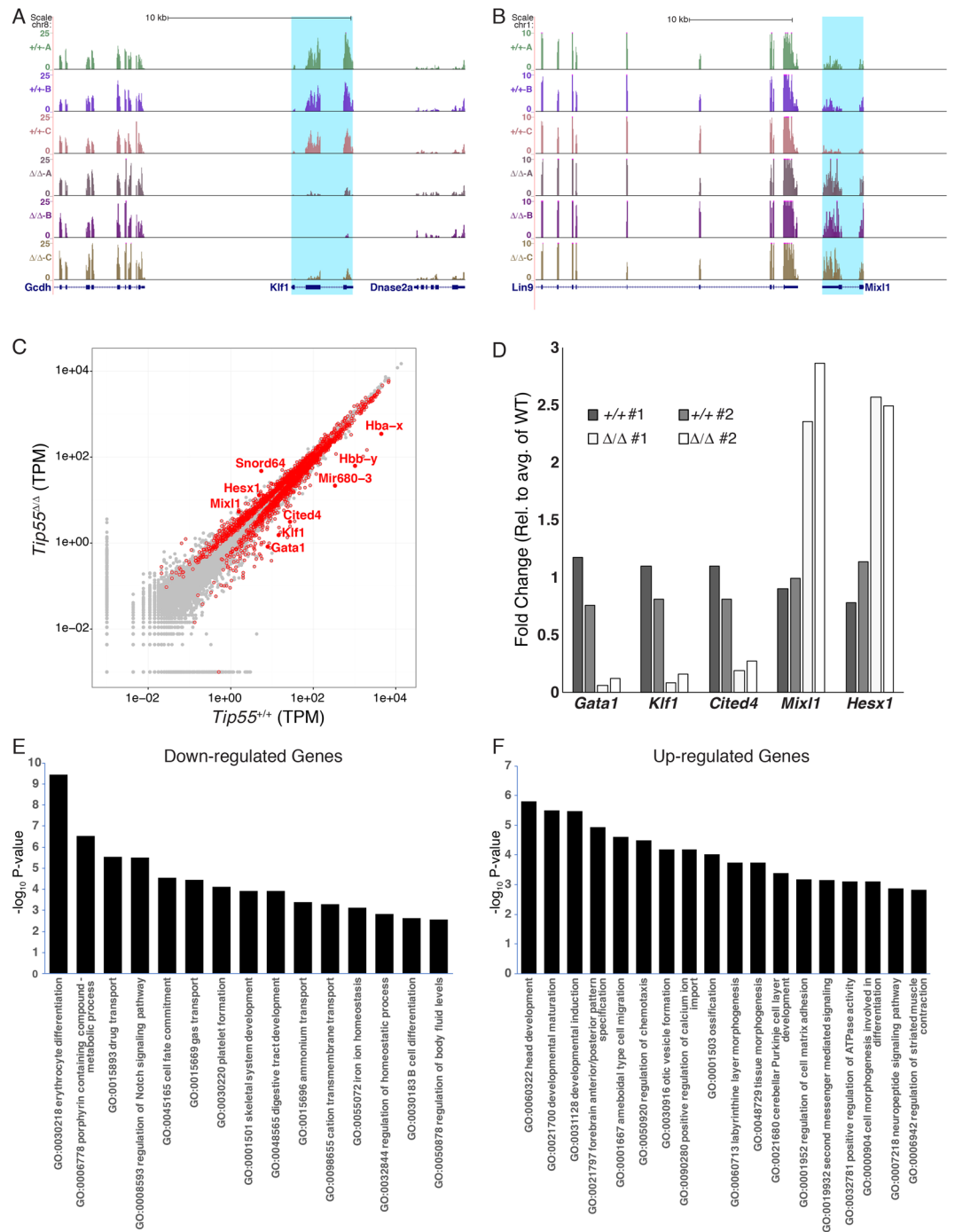


Figure 5. Genes necessary for organogenesis are misregulated in *Tip55* mutant embryos. **(A,B)** Browser tracks of developmental regulators (highlighted in blue) downregulated **(A)** or upregulated **(B)** in *Tip55*^{Δ/Δ} embryos (Δ/Δ) relative to *Tip55*^{+/+} embryos (+/+). Three biological replicate RNA-seq datasets (normalized for read number) for each genotype were performed. **(C)** Average transcripts per million (TPM) for each genotype are shown on a log-log scale with genes significantly differentially expressed in *Tip55*^{Δ/Δ} embryos (posterior probability of differential expression; PPDE > 0.95) highlighted with red circles. Several genes of interest labeled with solid red dots with gene names shown. **(D)** RT-qPCR validation of indicated genes from *Tip55*^{+/+} (+/+) or *Tip55*^{Δ/Δ} (Δ/Δ) E8.5 embryos. Genes were selected based on differential expression (up or downregulation) in RNA-seq experiments. Expression levels in biological duplicate *Tip55*^{+/+} or *Tip55*^{Δ/Δ} embryos are plotted individually, relative to the average of the *Tip55*^{+/+} (which is set to 1). **(E,F)** Significantly enriched gene ontology (GO) categories for genes down-regulated or up-regulated significantly (PPDE > 0.95) and $|\log_2$ (Fold Change)| > 0.6 are depicted in **(A)** and **(B)**, respectively.

types. Therefore, widespread developmental defects may result from poor proliferation or survival of cells that comprise multiple tissues. Alternatively, these cellular phenotypes may result from more complex developmental impairments owing to defects in the gene regulatory networks specific to each lineage.

The finding that *Tip55*, a poorly-studied splice variant of *Kat5*, plays specific roles in development raises the possibility that each of the other *Kat5* isoforms play non-redundant roles in development that have yet to be discovered. This raises a larger question regarding regulation of developmental gene expression in mammals – do additional chromatin regulatory enzymes that are expressed in multiple isoforms have distinct functions that are specific for each isoform? Although the functions of splice variants of a few mammalian chromatin regulatory enzymes have been addressed *in vitro*^{21,22}, the generation of isoform specific mutant animals will be necessary to assess their potential functions *in vivo*. Such studies have been performed in *Drosophila* for the SWI/SNF family ATPase, *domino*, in which two splice isoforms were found to function in distinct cell types²³. Although multiple isoforms of one of two mammalian homologs of *domino*, *Ep400*, have been identified, it remains to be tested whether they exhibit similar cell type specificity. Therefore, an effort to make and characterize isoform-specific alleles of numerous mammalian chromatin remodeling enzymes will likely provide important insights into developmental gene regulation.

Methods

Antibodies. Antibodies used in this study were as follows: H3S10P (9701, Cell Signaling Technologies), and Cleaved caspase 3 (9661, Cell Signaling Technologies).

Generation of *Tip55* knockout mice. All animal experiments were approved by the Institutional Animal Care and Use Committee of University of Massachusetts Medical School (approval number A-2165). All animal procedures were performed in accordance with UMMS and NIH guidelines on animal care. The mutant mouse line with the *Tip55* deletion is equivalent to the parental line in which the *Tip60^c* allele was generated by Cre mediated recombination of fused exons 11–14, placing a catalytically inactive version of exon 11 into the *Kat5* gene. This parental allele (prior to Cre mediated recombination) specifically lacks the *Tip55* isoform^{13,14}. Mice were genotyped by PCR with primers listed in Table S2. *Tip55^{Δ/+}* mice were maintained as heterozygotes on an inbred FVB/N background and intercrossed to generate *Tip55^{+/+}*, *Tip55^{Δ/+}* and *Tip55^{Δ/Δ}* embryos.

RNA *in situ* hybridization. Whole mount *in situ* hybridization of wild type embryos were performed as previously described²⁴. A unique region of *Tip55* cDNA (293 bases) was used to generate *Tip55* sense and anti-sense probes.

Derivation of MEFs. MEFs were generated from E9.5 embryos as previously described²⁵. Briefly, E9.5 embryos were dissected, and trypsin (0.05%) digested for 12 minutes at 37°C. Embryos were pipetted to obtain single cells and cultured in a 12 well plate in DMEM with 10% FBS.

Cell proliferation assays. MEFs from two independent embryos from each genotype (*Tip55^{+/+}*, *Tip55^{Δ/+}* and *Tip55^{Δ/Δ}*) were seeded at approximately 50% confluency and cultured in wells of a 12-well plate. The total number of cells were counted and re-plated into new 12-well plates every 48 hours for a total of four days to measure proliferation rate.

β-galactosidase staining. MEFs were isolated from E9.5 embryos and cultured in a 12-well plate. Three days after plating, cells were sub-cultured for an additional two days followed by staining for β-galactosidase activity using a kit (Millipore KAA002) according to manufacturer's protocol.

Hematoxylin and Eosin (H&E) Staining. E8.5 embryos were collected and sectioned at 8μm thickness for morphological analysis as previously described²⁶. Hematoxylin- and eosin- staining was performed by de-paraffinizing sections in xylene, rehydrating slides through an ethanol gradient, staining for 30 s with 30% Harris modified hematoxylin and a 30 s counterstain with eosin Y. Slides were rinsed and dehydrated with ethanol, cleared with xylene, and mounted using Vectashield mounting media.

Immunohistochemistry and Immunofluorescence. Sections from E8.5 embryos were examined for proliferation and apoptosis defects by immunohistochemistry, following protocols described previously²⁶. Briefly, sections were rehydrated through an ethanol gradient, followed by heat antigen retrieval (Buffer A, Electron Microscopy Sciences). Immunostaining was conducted using the Vectastain Elite ABC and DAB Peroxidase Substrate kit according to manufacturer guidelines. Sections were incubated with H3S10P (1:100; Cell signaling, CSG 9706) or cleaved caspase 3 (1:100; Cell signaling, CSG 9661) biotinylated primary antibodies overnight at 4°C²⁶. For counterstaining, slides were rinsed and then incubated with 30% hematoxylin for 30 s after developing staining with 3,3' diaminobenzimidine. All slides were ethanol-dehydrated, cleared with xylene, and mounted with Vectashield mounting medium.

Expression of cardiac and neural markers in embryonic sections was examined by immunofluorescence. E8.5 embryo sections were rehydrated, then subjected to heat antigen retrieval as described above. Sections were incubated with Sox2 antibody (1:200; R&D research, AF2018) from goat and cTNT antibody (1:50; DSHB, RV-C2) from mouse overnight at 4°C. The following secondary antibodies were used: Alexa 488 anti-goat (1:200; Life Technologies, A-11055) and Alexa 564 anti-mouse (1:500; Life Technologies, A-11037). Slides were mounted with Vectashield mounting media. Images were taken with a Nikon Eclipse 80i microscope and NIS-Elements 4.00.03 software.

Proliferation and Apoptosis Quantification. For quantification of H3S10P or cleaved caspase 3 immunostaining, digital images were taken using a Nikon Eclipse 80i microscope and the NIS-Elements 4.00.03 software. Positively stained cells were counted manually using ImageJ (v 1.6.0_65). The percentage of H3S10P positive or cleaved caspase-3 positive cells relative to the total number of nuclei was calculated for a minimum of three embryos per genotype.

RNA sequencing. RNA was isolated from E8.5 embryos using a Direct-zol RNA MicroPrep kit (Zymo research). Enrichment of mRNA, library preparation, and sequencing were performed at BGI, using the BGI-seq format. Reads were mapped to the mm10 genome and quantified using RSEM²⁷. Identification of differentially expressed genes was performed using a combined RSEM-EBseq pipeline²⁰. Gene ontology enrichment was performed using Metascape (<http://metascape.org>)²⁸.

Data Availability

Sequence reads for all RNA-seq libraries have been deposited at Gene Expression Omnibus (GEO) and are available with accession number: GSE111691.

References

- Guertin, M. J. & Lis, J. T. Mechanisms by which transcription factors gain access to target sequence elements in chromatin. *Curr Opin Genet Dev* **23**, 116–123 (2013).
- Villar, D., Flicek, P. & Odom, D. T. Evolution of transcription factor binding in metazoans — mechanisms and functional implications. *Nat Rev Genet* **15**, 221–233 (2014).
- Gonzalez-Sandoval, A. & Gasser, S. M. On TADs and LADs: Spatial Control Over Gene Expression. *Trends Genet.* **32**, 485–495 (2016).
- Mirabella, A. C., Foster, B. M. & Bartke, T. Chromatin deregulation in disease. *Chromosoma* **125**, 75–93 (2015).
- Tang, Y., Luo, J., Zhang, W. & Gu, W. Tip60-dependent acetylation of p53 modulates the decision between cell-cycle arrest and apoptosis. *Mol Cell* **24**, 827–839 (2006).
- Sykes, S. M. *et al.* Acetylation of the p53 DNA-binding domain regulates apoptosis induction. *Mol Cell* **24**, 841–851 (2006).
- Sun, Y., Jiang, X., Chen, S., Fernandes, N. & Price, B. D. A role for the Tip60 histone acetyltransferase in the acetylation and activation of ATM. *Proc Natl Acad Sci USA* **102**, 13182–13187 (2005).
- Ikura, T. *et al.* Involvement of the TIP60 histone acetylase complex in DNA repair and apoptosis. *Cell* **102**, 463–473 (2000).
- Yamamoto, T. & Horikoshi, M. Novel substrate specificity of the histone acetyltransferase activity of HIV-1-Tat interactive protein Tip60. *J Biol Chem* **272**, 30595–30598 (1997).
- Squatrito, M., Gorrini, C. & Amati, B. Tip60 in DNA damage response and growth control: many tricks in one HAT. *Trends in Cell Biology* **16**, 433–442 (2006).
- Kusch, T. *et al.* Acetylation by Tip60 is required for selective histone variant exchange at DNA lesions. *Science* **306**, 2084–2087 (2004).
- Legube, G. *et al.* Role of the histone acetyl transferase Tip60 in the p53 pathway. *J Biol Chem* **279**, 44825–44833 (2004).
- Acharya, D. *et al.* KAT-Independent Gene Regulation by Tip60 Promotes ESC Self-Renewal but Not Pluripotency. *Cell Reports* **19**, 671–679 (2017).
- Chen, P. B. *et al.* Hdac6 regulates Tip60-p400 function in stem cells. *Elife* **2**, e01557 (2013).
- Fazio, T. G., Huff, J. T. & Panning, B. An RNAi screen of chromatin proteins identifies Tip60-p400 as a regulator of embryonic stem cell identity. *Cell* **134**, 162–174 (2008).
- Hu, Y. *et al.* Homozygous disruption of the Tip60 gene causes early embryonic lethality. *Dev Dyn* **238**, 2912–2921 (2009).
- Kim, M.-S., Merlo, X., Wilson, C. & Lough, J. Co-activation of atrial natriuretic factor promoter by Tip60 and serum response factor. *J Biol Chem* **281**, 15082–15089 (2006).
- Legube, G. & Trouche, D. Identification of a larger form of the histone acetyl transferase Tip60. *Gene* **310**, 161–168 (2003).
- Ran, Q. & Pereira-Smith, O. M. Identification of an alternatively spliced form of the Tat interactive protein (Tip60), Tip60(beta). *Gene* **258**, 141–146 (2000).
- Leng, N. *et al.* EBSeq: an empirical Bayes hierarchical model for inference in RNA-seq experiments. *Bioinformatics* **29**, 1035–1043 (2013).
- Zibetti, C. *et al.* Alternative Splicing of the Histone Demethylase LSD1/KDM1 Contributes to the Modulation of Neurite Morphogenesis in the Mammalian Nervous System. *Journal of Neuroscience* **30**, 2521–2532 (2010).
- Barak, O., Lazzaro, M. A., Cooch, N. S., Picketts, D. J. & Shiekhattar, R. A Tissue-specific, Naturally Occurring Human SNF2L Variant Inactivates Chromatin Remodeling. *J Biol Chem* **279**, 45130–45138 (2004).
- Börner, K. & Becker, P. B. Splice variants of the SWR1-type nucleosome remodeling factor Domino have distinct functions during *Drosophila melanogaster* oogenesis. *Development* **143**, 3154–3167 (2016).
- Rivera-Pérez, J. A. & Magnuson, T. Primitive streak formation in mice is preceded by localized activation of Brachyury and Wnt3. *Dev Biol* **288**, 363–371 (2005).
- Todaro, G. J. & Green, H. Quantitative studies of the growth of mouse embryo cells in culture and their development into established lines. *J. Cell Biol.* **17**, 299–313 (1963).
- Milstone, Z. J., Lawson, G. & Trivedi, C. M. Histone deacetylase 1 and 2 are essential for murine neural crest proliferation, pharyngeal arch development, and craniofacial morphogenesis. *Dev Dyn* **246**, 1015–1026 (2017).
- Li, B. & Dewey, C. N. RSEM: accurate transcript quantification from RNA-Seq data with or without a reference genome. *BMC Bioinformatics* **12**, 323 (2011).
- Tripathi, S. *et al.* Meta- and Orthogonal Integration of Influenza “OMICs” Data Defines a Role for UBR4 in Virus Budding. *Cell Host and Microbe* **18**, 723–735 (2015).

Acknowledgements

We thank K. McCannell, T. Wu, and J. Benanti for critical comments on the manuscript. This work was supported by the National Institutes of Health [R01HD072122 to T.G.F.; R01HL118100 to C.M.T.; and R01HD083311 to J.A.R.-P.] and the American Cancer Society [RSG-14-220-01] to T.G.F. B.N. was supported by a Translational Cancer Biology Postdoctoral training grant from the NIH (T32CA130807). T.G.F. is a Leukemia and Lymphoma Society Scholar.

Author Contributions

D.A. and B.N. performed initial characterization of the Tip55 mutant and most experiments. Z.J.M. and L.B. performed IHC experiments with assistance from C.M.T. Y.Y. and B.N. performed *in situ* hybridizations with assistance from J.A.R.-P. D.A. and T.G.F. analyzed RNA-seq data. D.A., B.N., and T.G.F. wrote the manuscript with input from all authors.

Additional Information

Supplementary information accompanies this paper at <https://doi.org/10.1038/s41598-018-33213-4>.

Competing Interests: The authors declare no competing interests.

Publisher's note: Springer Nature remains neutral with regard to jurisdictional claims in published maps and institutional affiliations.



Open Access This article is licensed under a Creative Commons Attribution 4.0 International License, which permits use, sharing, adaptation, distribution and reproduction in any medium or format, as long as you give appropriate credit to the original author(s) and the source, provide a link to the Creative Commons license, and indicate if changes were made. The images or other third party material in this article are included in the article's Creative Commons license, unless indicated otherwise in a credit line to the material. If material is not included in the article's Creative Commons license and your intended use is not permitted by statutory regulation or exceeds the permitted use, you will need to obtain permission directly from the copyright holder. To view a copy of this license, visit <http://creativecommons.org/licenses/by/4.0/>.

© The Author(s) 2018